





Familial primary ovarian insufficiency associated with an *SYCE1* point mutation: defective meiosis elucidated in humanized mice

Diego Hernández-López¹, Adriana Geisinger^{1,2},
María Fernanda Trovero³, Federico F. Santinaque⁴, Mónica Brauer⁵,
Gustavo A. Folle^{3,4}, Ricardo Benavente ^{6,*}, and
Rosana Rodríguez-Casuriaga ^{1,2,*}

¹Department of Molecular Biology, Instituto de Investigaciones Biológicas Clemente Estable (IIBCE), 11600 Montevideo, Uruguay ²Biochemistry-Molecular Biology, Facultad de Ciencias, Universidad de la República (UdelaR), 11400 Montevideo, Uruguay ³Department of Genetics, IIBCE, 11600 Montevideo, Uruguay ⁴Flow Cytometry and Cell Sorting Core, IIBCE, 11600 Montevideo, Uruguay ⁵Laboratory of Cell Biology, Department of Experimental Neuropharmacology, IIBCE, 11600 Montevideo, Uruguay ⁶Department of Cell and Developmental Biology, Biocenter, University of Würzburg, D-97074 Würzburg, Germany

*Correspondence address. Department of Molecular Biology, Instituto de Investigaciones Biológicas Clemente Estable (IIBCE), 11.600 Montevideo, Uruguay. E-mail: rrodriguez@iibce.edu.uy;  orcid.org/0000-0002-7656-0288; Department of Cell and Developmental Biology, Biocenter, University of Würzburg, D-97074 Würzburg, Germany. E-mail: benavente@biozentrum.uni-wuerzburg.de;  orcid.org/0000-0001-6361-0672

Submitted on February 12, 2020; resubmitted on April 24, 2020; editorial decision on May 6, 2020

ABSTRACT: More than 50% of cases of primary ovarian insufficiency (POI) and nonobstructive azoospermia in humans are classified as idiopathic infertility. Meiotic defects may relate to at least some of these cases. Mutations in genes coding for synaptonemal complex (SC) components have been identified in humans, and hypothesized to be causative for the observed infertile phenotype. Mutation *SYCE1* c.721C>T (former c.613C>T)—a familial mutation reported in two sisters with primary amenorrhea—was the first such mutation found in an SC central element component-coding gene. Most fundamental mammalian oogenesis events occur during the embryonic phase, and eventual defects are identified many years later, thus leaving few possibilities to study the condition's etiology and pathogenesis. Aiming to validate an approach to circumvent this difficulty, we have used the CRISPR/Cas9 technology to generate a mouse model with an *SYCE1* c.721C>T equivalent genome alteration. We hereby present the characterization of the homozygous mutant mice phenotype, compared to their wild type and heterozygous littermates. Our results strongly support a causative role of this mutation for the POI phenotype in human patients, and the mechanisms involved would relate to defects in homologous chromosome synapsis. No *SYCE1* protein was detected in homozygous mutants and *Syce1* transcript level was highly diminished, suggesting transcript degradation as the basis of the infertility mechanism. This is the first report on the generation of a humanized mouse model line for the study of an infertility-related human mutation in an SC component-coding gene, thus representing a proof of principle.

Key words: gametogenesis / idiopathic infertility / primary ovarian insufficiency / meiosis / synaptonemal complex / *SYCE1* / CRISPR/Cas9 / humanized mice

Introduction

Primary ovarian insufficiency (POI) is a clinical syndrome characterized by loss of ovarian activity before the age of 40 years. It is a heterogeneous condition with a broad phenotypic spectrum, sharing the common feature of ovarian follicle dysfunction or follicle depletion. It can have serious noxious effects upon women's psychological and physical

health. POI incidence increases with age, affecting one in every 10 000 women at the age of 20 years, and 1 in 100 at the age of 40 years (Goswami and Conway, 2005). Most cases (50–90%) have unknown causes and, therefore, are classified as idiopathic (Chapman *et al.*, 2015). An important number of idiopathic POI cases have been related to the genetic background of the diagnosed females (Coulam *et al.*, 1983), with 10–15% of them having an affected first-degree

relative (Van Kasteren and Schoemaker, 1999). Among the already reported causes of POI are alterations in chromosome number and structure (e.g. Turner's syndrome, 45,X) as well as genomic changes in 46,XX nonsyndromic patients (Fonseca et al., 2015; Laissue, 2015; Huhtaniemi et al., 2018). During the last two decades, an increasing number of POI-associated genes have been identified both on the X chromosome (e.g. Riva et al., 1996; Di Pasquale et al., 2006; Ennis et al., 2006; Laissue et al., 2006) and in autosomes (e.g. Doherty et al., 2002; Laissue et al., 2006; Watkins et al., 2006; Qin et al., 2007; Zhao et al., 2008), as well as in mitochondrial DNA (Pagnamenta et al., 2006), thus confirming the heterogeneous nature of the genetic causal component.

Given the requirement of meiotic divisions for normal gamete formation, it is expected that mutations in meiosis-related genes would account for at least part of the idiopathic infertility cases. Specifically, since synaptonemal complexes (SCs) are essential structures for recombination and proper chromosome segregation (and thus for gametogenesis progression), alterations in SC-coding genes are obvious candidates to be causative for infertility (revised by Geisinger and Benavente, 2016), and particularly of POI. The SC is a meiosis-specific proteinaceous, ladder-like structure that physically binds together homologous chromosomes and facilitates the resolution of recombination intermediates (Zickler and Kleckner, 2015). SCs are composed of two lateral elements (LEs), a central element (CE) and transverse filaments (TFs) linking both LEs with the CE. The CE together with the TFs constitutes the SC central region (CR). So far, eight different SC protein components have been identified, including LE proteins SYCP3 (Lammers et al., 1994; Alsheimer et al., 2010) and SYCP2 (Offenberg et al., 1998; Yang et al., 2006; Winkel et al., 2009), TF constituent SYCP1 (Meuwissen et al., 1992; De Vries et al., 2005; Schücker et al., 2015) and CE components SYCE1, SYCE2, SYCE3, TEX12 and SIX6OS (Costa et al., 2005; Hamer et al., 2006; Schramm et al., 2011; Gómez-H et al., 2016).

The involvement of SC components in POI would be supported by loss-of-function studies for different SC genes employing knockout (KO) mice, which have been reported to disrupt SC structure, and lead to infertility (reviewed by Yuan et al., 2002; De Vries et al., 2005; Yang et al., 2006; Bolcun-Filas et al., 2007; Hamer et al., 2008; Bolcun-Filas et al., 2009; Schramm et al., 2011; Fraune et al. 2012; Gómez-H et al., 2016). Some human mutations in SC-coding genes have been identified and linked to infertility as well (reviewed by Geisinger and Benavente, 2016). Concerning LE components, various mutations for SYCP3 have been reported, and the first SYCP2 mutations have recently been identified (Schilit et al., 2020).

Regarding CE components of the SC, in recent years mutations potentially associated with clinical conditions have started to be reported. In particular, deletions in human 10q26.3 encompassing the *SYCE1* gene were found in patients with POI (McGuire et al., 2011; Zhen et al., 2013; Bestetti et al., 2019). Very recently, a consanguineous familial study led to the identification of a homozygous gross deletion affecting ~4000 bp of *SYCE1* that was associated to POI (Zhe et al., 2020). Besides, thus far three reports identifying mutations in *SYCE1* in infertile patients have been made, all of them from consanguineous families (de Vries et al., 2014; Maor-Sagie et al., 2015; Pashaei et al., 2020). In the first of these reports, a homozygous point mutation was identified in a 13-member-family in which two sisters born to consanguineous parents suffered primary amenorrhea (de Vries et al., 2014). This mutation—initially identified as *SYCE1* c.613C>T—corresponds

to *SYCE1* c.721C>T (GRCh38.p13 human genome release), and would lead to *SYCE1* protein truncation. By sequencing studies, the authors determined that of the 11 descendants (five males and six females), only the two affected siblings were homozygous for the *SYCE1* c.721C>T point mutation, suggesting a genetic cause with a recessive mode of inheritance (de Vries et al., 2014). Although the idea of a possible relation of *SYCE1* mutation with pathogenesis would be supported by the phenotype of *Syce1* KO mice, which are infertile (Bolcun-Filas et al., 2009), an unequivocal evaluation linking *SYCE1* mutations to the observed medical conditions is lacking.

As most fundamental mammalian oogenesis events (including SC formation and recombination) occur during the embryonic phase, eventual defects in this process are only identified after many years of delay, leaving few possibilities to intervene, and even to study the condition's etiology and pathogenesis. A valid alternative to circumvent this difficulty is the employment of suitable animal models, which has the highest physiological relevance after human studies. So far, some mouse models have been generated for the study of putative infertility-linked alleles in genes involved in meiotic double-strand break (DSB) repair and recombination pathways (Tran and Schimenti, 2018, 2019; Tran et al., 2019). However, thus far no transgenic humanized mice mimicking mutations found in humans for any SC component-coding gene have been reported.

In order to evaluate a causative role of mutation *SYCE1* c.721C>T in the observed infertile phenotype, and to study its pathogenesis, we have generated a humanized mouse model line containing an equivalent point mutation by using the clustered regularly interspaced short palindromic repeats/CRISPR-associated protein 9 (CRISPR/Cas9) mutagenesis system. Here, we present the phenotypic characterization of the humanized mutant mice, helping to shed light on the etiology and mechanisms of these infertility cases. We also discuss the potential usefulness of these humanized mouse models as substrates for future development of gene therapy approaches.

Materials and methods

Ethical approval

All animal procedures to generate the mutant line were performed at the SPF animal facility of the Transgenic and Experimental Animal Unit of Institut Pasteur de Montevideo. Experimental protocols were accordingly approved by the institutional Animal Ethics Committee (protocol number 007-18), in accordance with National Law of animal experimentation 18,611 (Uruguay) and international animal care guidelines (Guide for the Care and Use of Laboratory Animals) (National Research Council (NRC), 1996).

All subsequent experimental animal procedures were performed at Instituto de Investigaciones Biológicas Clemente Estable (IIBCE, Montevideo, Uruguay), also in accordance with National Law 18,611, and following the recommendations of the Uruguayan National Commission of Animal Experimentation (CNEA, approved experimental protocol 009/11/2016).

Design of molecules for mutagenesis

CRISPR/Cas mutagenesis was employed aiming to obtain a humanized mouse cell line with an equivalent point mutation to the human *SYCE1*

gene c.721C>T (former SYCE1 c.613C>T, de Vries et al., 2014), which in mouse corresponds to *Syce1* c.727C>T. Design and selection of molecules to be used in the directed mutagenesis were carried out taking into account on-target ranking, off-target ranking and distance of single-guide RNA (sgRNA) to target site of mutagenesis (<http://www.broadinstitute.org/rnai/public/analysis-tools/sgna-design>). The selected sgRNA was acquired as CRISPR*Evolution Synthetic sgRNA kit* (Synthego, USA). The single-stranded oligonucleotide donor employed as template for homology-directed repair (HDR) was designed making use of online tools for silent mutation scanning (<http://watcut.uwaterloo.ca/template.php>) and restriction enzyme analysis (nc2.neb.com/NEBcutter2/), and ordered from IDT as 4 nmole Ultramer DNA Oligo (IDT, USA). Protospacer adjacent motif was disrupted in the single-stranded donor oligonucleotide (ssODN) in order to avoid repeated nuclease action after eventual correction.

Mice manipulation for genome editing

Mice were housed in individually ventilated cages (Tecniplast, Milan, Italy), in a controlled environment at 20°C ± 1°C with a relative humidity of 40–60%, in a 14/10 h light-dark cycle. Autoclaved food (Labdiet 5K67, PMI Nutrition, USA) and water were administered *ad libitum*.

Cytoplasmic microinjection was performed in C57BL/6J zygotes using a mix of 20 ng/μl sgRNA, 30 ng/μl Cas9 mRNA and 20 ng/μl ssDNA oligo. The same day, surviving zygotes were transferred to oviducts of B6D2F1 0.5 day postcoitum pseudopregnant females (25 embryos/female in average), following surgery procedures established in the animal facility (Crispo et al., 2013). Previously, recipient females were anesthetized with a mixture of ketamine (100 mg/kg, Pharmaservice, Ripoll Vet, Uruguay) and xylazine (10 mg/kg, Seton 2%; Calier, Uruguay). Tolfenamic acid was administered s.c. (1 mg/kg, Tolfedine, Vetoquinol, Spain) in order to provide analgesic and anti-inflammatory effects (Schlapp et al., 2015). Pregnancy diagnosis was determined by visual inspection by an experienced animal caretaker 2 weeks after embryo transfer, and litter size was recorded when the litters were 21 days old.

Genotyping of transgenic mice

Offspring genotyping was performed *via* tail-tips. DNA was extracted by means of *GeneJET Genomic DNA Purification Kit* (Thermo Fisher Scientific, USA). The genomic region of interest (i.e. where the mutation was directed) was specifically amplified by standard PCR. The primers employed were:

Syce1-727-FOR: 5'-TCAAGGAAGGTGAGGTCAGG-3';

Syce1-727-REV: 5'-ATGAAGAGACATACCGGCAG-3'.

PCR products were run by electrophoresis, recovered by the *GeneJET Gel Extraction and DNA Cleanup Micro Kit* (Thermo Fisher Scientific, USA), and sequenced.

Fertility tests

Fertility was assessed both for females and males by mating 2-month-old mutant mice homozygous for the change with adult wild type (WT) mice of opposite gender. Heterozygous mutants and WT mice were used as control groups. Assays were performed in triplicate for each gender in breeding pairs or trios (two females and one male).

After a period of at least 3 months without offspring, the analyzed mice were considered infertile.

Histology

Whole adult testes and ovaries were primary fixed in 2.5% glutaraldehyde, postfixed in 1% osmium tetroxide, dehydrated and resin-embedded (Durcupan ACM, Fluka, Sigma-Aldrich, USA) according to conventional procedures (Glauert and Lewis, 1998). Thereafter, 250 nm sections were cut using a *Power Tome XL* ultra-microtome (Boeckeler Instruments, USA), stained with toluidine blue, and examined by bright field microscopy. Photographs were taken by means of an *Olympus FV300* microscope equipped with a *DP70* camera, and *DPController v.1.1.1.65* software (Olympus, Tokyo, Japan).

Analysis by flow cytometry

Testicular cell suspensions were prepared using a mechanical method previously described by our group (Rodríguez-Casuriaga et al., 2009, 2013). The resulting cell suspensions were stained with Vybrant DyeCycle Green (VDG, Invitrogen Life Technologies, USA) at a final concentration of 10 μM for 1 h at 35°C in the dark with gentle agitation (80 rpm), as reported earlier (Rodríguez-Casuriaga et al., 2014).

Flow cytometry (FCM) analyses were performed by means of a flow cytometer and cell sorter *MoFlo Astrios EQ* (Beckman Coulter, USA), using a 488 nm laser, a 100 μm nozzle (25 psi) and Summit software (Beckman Coulter, IN, USA). Flow cytometer calibration and quality control were carried out using *3.0 μm Ultra Rainbow Fluorescent Particles* (Spherotech, USA). Fluorescence emitted from VDG was detected with a 513/26 bandpass filter. The following parameters were analyzed: forward scatter (FSC-Height with PI Mask), side scatter (SSC-Height), 513/26-Area (VDG fluorescence intensity) and 513/26-Width. Doublets were excluded using dot plots of 513/26 pulse-area versus 513/26 pulse-width. FCM data were analyzed with Kaluza software (Beckman Coulter, IN, USA).

Antibodies

A primary antibody against SYCE1 amino-terminal region (i.e. capable of detection of WT SYCE1 and its putative truncated form) was developed at GenScript (GenScript USA Inc.). In order to achieve this, peptides ATRPQPLGMEPEGSC and CPEGARGQYGSTQKI from the amino-terminal part of the protein were conjugated to KLH, and employed as immunogens in New Zealand rabbits. The affinity-purified antibody was employed both for fluorescence microscopy (1:200) and in western blots (0.3 μg/ml).

Guinea pig anti-SYCP3 (1:200), guinea pig anti-TEX12 (1:200), rabbit anti-SYCP1 (1:200) and rabbit anti-SYCE3 (1:200) primary antibodies were used as affinity-purified immunoglobulins and described in detail elsewhere (Schücker et al., 2015). Mouse anti-γH2AX (histone) was purchased at Millipore (1:500, 05-636; Millipore, Germany).

The primary antibody anti-β-tubulin—employed in western blots as loading control—was acquired from Abcam (ab6046, 1:8000, Abcam Antibodies, USA), and revealed using an anti-rabbit secondary antibody coupled to horse-radish peroxidase (1:30 000, Pierce, Thermo Fisher Scientific, USA).

Suitable secondary antibodies coupled to AlexaFluor dyes were acquired from Invitrogen Life Technologies, USA: AlexaFluor488 goat anti-

rabbit (A11034, 1:1000), AlexaFluor633 goat anti-guinea pig (A21105, 1:1000) and AlexaFluor546 goat anti-guinea pig (A11074, 1:1000).

Immunocytochemistry

Immunolocalization assays were performed on gonadal spread cells obtained through the dry-down technique (Peters et al., 1997) with minor modifications. Briefly, for oocyte spreading, fetal ovaries (E18 embryos) were dissected, incubated in hypotonic buffer (30 mM Tris-HCl pH 8.2, 17 mM sodium citrate, 5 mM EDTA, 50 mM sucrose, 5 mM dithiothreitol) for 30 min, mechanically disaggregated on clean slides containing 100 mM sucrose, fixed in 1%-paraformaldehyde/0.15%-TritonX100 and allowed to dry slowly (overnight in closed humidity chamber, then open). Once completely dry, slides were wrapped in aluminum foil, and stored at -80°C until use. For spermatocyte spreading, the same procedure was applied on mechanically disaggregated adult mice testes.

Slides were afterwards used for incubations with the indicated antibodies for immunofluorescence microscopy. All incubations with primary antibodies were performed overnight at 4°C in the presence of protease inhibitors (P2714, Sigma-Aldrich, USA). Secondary antibody incubations were done at room temperature for 1 h protected from light.

Microscopy and imaging

All immunofluorescence microscopy acquisitions were performed employing a Zeiss LSM 800 confocal microscope (Carl Zeiss Microscopy, Germany) equipped with an Airyscan processing module, a 63X/1.4 N.A. Plan Achromat oil objective, AxioCam 506 color digital camera and ZEN Blue 2.3 software (Carl Zeiss Microscopy, Germany). Airyscan image processing was done through the software's automatic deconvolution step. All image analyses were performed by means of Fiji ImageJ software (Schindelin et al., 2012).

Statistical analyses

Quantitative data from spread nuclei with synapsed chromosomes (zygotene and pachytene stage) from homozygous and heterozygous mutants with WT littermate controls were statistically compared using a chi-square test. Regarding quantitative RT-PCR (qRT-PCR) and fluorescence intensity data, statistical significance and *P*-value were calculated in R bioconductor (<http://cran.r-project.org/>).

Western blots

Testicular protein lysates corresponding to 7.5×10^5 cells in Laemmli sample buffer were loaded per lane. Sodium dodecyl sulfate-polyacrylamide gel electrophoresis was carried out on 12% polyacrylamide gels. Protein gels were transferred to nitrocellulose membranes as instructed (Matsudaira, 1987), and western blots were performed as previously described (Goldman et al., 2015). Membranes were incubated for 2 h at room temperature in Tris-buffered saline/0.1%-Tween20 with primary antibodies: (anti-SYCE1-Nt and anti- β -tubulin), and for 1 h in blocking solution with anti-rabbit secondary antibody. Bound antibodies were detected by using the Super Signal West Pico substrate (Pierce, Thermo Fisher Scientific, USA). All assays were performed more than once, and using biological replicates.

qRT-PCR assays

Total RNA from testicular cell suspensions was extracted with PureLink RNA Mini Kit (Ambion, Thermo Fisher Scientific, USA), following manufacturer's recommendations. RNA quantification was done by Nanodrop 1000 Spectrophotometer (Thermo Fisher Scientific, USA). Retro-transcription and qPCR were performed using Power SYBR Green Cells-to-Ct kit (Ambion, Thermo Fisher Scientific, USA), starting from 50 ng of RNA, following kit instructions, in a CFX96 Touch Real-Time PCR Detection System 1 (BioRad, USA). For qPCR step, 2 μl cDNA in 20 μl final volume reaction mix was used.

For qRT-PCR on embryonic ovaries, the same kit was directly employed after a lysis reaction with no previous RNA extraction (due to the scarcity of the tissue).

The primers used are listed in Supplementary Table S1. We made three biological replicas, and chose *Ppp1cc* (protein phosphatase 1, catalytic subunit, gamma isozyme) as normalizing gene, as it has been previously shown to be a good normalizing gene for testicular RNA (da Cruz et al., 2016). Amplification efficiency of all primers was $>93\%$. The $2^{-\Delta\Delta\text{Ct}}$ method and WT mouse RNA as calibrator condition were used (Livak and Schmittgen, 2001).

Results

Generation of model mouse line

Our first aim was to generate a model mouse line mimicking the SYCE1 c.721C>T point mutation observed in humans. To achieve this, we chose to use CRISPR/Cas9 technology, and proceeded as described in Materials and methods section. Comparison of SYCE1 coding regions from human and mouse genome revealed high identity, thus facilitating the choice of the editing target (Fig. 1A). SYCE1 c.721C>T is a nonsense mutation that would lead to a truncated human SYCE1 protein of 240 residues, while its WT counterpart has 351 amino acids. In mouse, an equivalent mutation would lead to a truncated protein of 242 amino acids, as compared to the WT 329-residue version.

Design of molecules to be used in the directed mutagenesis (sgRNA and ssODN) was optimized to favor the HDR pathway (Fig. 1B) (Yang et al., 2013). Specimens resulting from microinjected zygotes (F0) were genotyped in search of the desired change, and then mated with WT mice to obtain the F1 generation. Afterwards, heterozygous specimens from F1 were intermated to generate F2 offspring: as expected, the latter included WT specimens as well as others heterozygous and homozygous for the desired point mutation, which in mouse corresponds to *Syce1* c.727C>T (Fig. 1C).

Syce1 c.727C>T homozygous mutation causes infertility both in female and male mice

Fertility was assessed both for females and males by mating mutant mice with WT specimens of opposite gender. Data from three experimental groups were compared in these studies: WT, heterozygous and homozygous mice. No differences were observed between WT and heterozygous mice, which easily became pregnant, and had on average seven pups with an equal ratio of male and female offspring.

After a period of 3 months, only mice homozygous for the *Syce1* c.727C>T mutation failed to have offspring. This result was consistently reproduced in triplicates for each gender.

Syce1 c.727C>T homozygous mutation affects gonadal development

When gonadal size and aspect were assessed, no evident differences were found between adult WT and heterozygous mutant mice, neither for females nor for males (Supplementary Fig. S1A). However, adult homozygous mutants showed striking differences in gonadal size and aspect as compared to their WT littermates, and this proved to be true both for female and male adult mice (Fig. 1D).

Concerning microscopic analysis of ovaries, growing oocytes and follicle development was evident in adult WT and heterozygous female animals (Fig. 1E and Supplementary Fig. S1B). Morphological comparison between WT and heterozygous ovaries was performed by two experienced researchers on blind (unidentified) sections from three different specimens per condition (five sections from each specimen), and they were unable to distinguish one condition from the other. On the contrary, homozygous *Syce1* c.727C>T females presented minute ovaries with deeply altered histology, and lack of recognizable follicles or oocytes (Fig. 1E and Supplementary Fig. S2).

Regarding testicular development, while both WT and heterozygous adult males showed normal seminiferous tubules with complete spermatogenesis (Fig. 1E and Supplementary Fig. S1C), the microscopic analysis of gonadal content from adult homozygous male mutant mice revealed a severely affected spermatogenesis process, with complete absence of postmeiotic stages (Fig. 1E). The seminiferous tubules of these mutants were also depleted from mid and advanced prophase I stages (i.e. pachytene and diplotene), indicating an arrest in early meiotic prophase I stages. Moreover, the seminiferous tubules were much smaller than those of the WT and heterozygous mutants, and exhibited an immature aspect (Fig. 1E).

In order to have stronger quantitative comparative analyses, testicular cell suspensions from adult mice were analyzed by FCM, mainly based on DNA content (C, 2C and 4C populations). Figure 1F shows representative FCM results. While no significant differences were found between WT and heterozygous mutants, this study confirmed for the homozygous mutant males the complete absence of postmeiotic stages (i.e. spermatids with DNA content = C). Regarding the 4C population (mainly composed of primary spermatocytes), the FCM analyses hereby presented were obtained using the DNA-specific fluorochrome VDG that—as we had previously reported—allows the discrimination of two populations of spermatocytes: the early spermatocyte population (leptotene and zygotene stages, L/Z), and the mid/late spermatocyte one (pachytene and diplotene stages, P/D) (Rodríguez-Casuriaga et al., 2014). Although L/Z and P/D spermatocyte populations are usually visualized in the histograms of immature mice as a 4C bimodal peak (Supplementary Fig. S3A), the latter could not be observed in the FCM profiles from homozygous mutants (Fig. 1F) that resembled those expected for 13–14 days postpartum (dpp) WT juvenile mice, still lacking pachytene spermatocytes (Supplementary Fig. S3B) (Geisinger and Rodríguez-Casuriaga, 2017).

Evaluation of chromosome synapsis and SC assembly

The dramatic effect of the point mutation on gonadal development prompted us to study its consequences on SC structure and homologous chromosome synapsis. Immunocytochemical localizations were performed on spread cells from both embryonic ovaries and adult testes, and analyzed by confocal laser scanning microscopy.

A first set of studies was centered on SYCP3, in order to evaluate the differences between WT and mutants concerning SC LE spatial arrangement and chromosome synapsis. As the pachytene stage (completely synapsed homologs) is reached by Day 13–14 postpartum in male mice and by Day 17.5–18 postcoitum in female mice embryos, the ages of the specimens to be analyzed were chosen accordingly. Frequency data of spread meiotic nuclei with synapsed chromosomes from *Syce1* c.727C>T mutants and WT littermate controls were statistically compared using a chi-square test (χ^2). Once again, no evident differences were found between heterozygous mutants and WT littermates (χ^2 [1, $N=84$] = 0.26, $P=0.61$), with both presenting normal-looking spread chromosomes that had reached the pachytene stage (Fig. 2A). However, homozygous mutants consistently showed, at most, closely juxtaposed chromosomes that resembled earlier meiotic prophase stages, and we have considered this homolog arrangement asynapsis (Fig. 2A). These findings proved to be true for both genders (herein shown for females), and indicate that the homozygous presence of the point mutation severely affects homologous chromosome synapsis (χ^2 [1, $N=84$] = 134.6, $P<0.00001$), and would most probably account for the observed gametogenesis failure. SYCP3 fluorescence quantification on these preparations rendered no significant differences between WT and mutant mice ($P>0.1$).

As mentioned above, *Syce1* c.727C>T is a nonsense mutation that would lead to a truncated protein of 242 amino acids, as compared to the WT 329-residue version. In order to evaluate the eventual presence of the putative truncated SYCE1 protein in the SC of mutants, we investigated protein immunolocalization employing an antibody specially developed against peptides from SYCE1 amino-terminal (N-t) region (see Materials and Methods section). We clearly detected SYCE1 in spread meiotic nuclei from WT and heterozygous mutant mice, but not in those of homozygous mutants. This result was observed for both genders (herein shown for females; Fig. 2B), and was consistently obtained for all biological and technical replicates. Concerning SYCE1 fluorescence quantification, no significant differences were found between WT and heterozygous mutant mice ($P>0.1$).

Afterwards, we evaluated the presence of other known protein components of the SC CR (i.e. TFs and CE). Some have been reported to be loaded earlier than SYCE1 onto the SC (i.e. TF SYCP1 and CE SYCE3), while others would be loaded later (e.g. CE TEX12) (Fraune et al., 2012). Representative results are shown in Fig. 3. Again, no differences were found between WT and heterozygous mutants for any of the analyzed components either in female (Fig. 3A–C) or male meiotic nuclei (e.g. Fig. 3D). Regarding homozygous mutants, protein components SYCP1 and SYCE3 were detected on spread meiotic nuclei containing SCs in the assembling process (Fig. 3A and B), while TEX12 was not detected at all in the assembling structure (Fig. 3C and D). Concerning quantification, again no significant differences were found between WT and heterozygous mutant mice. On the contrary, both

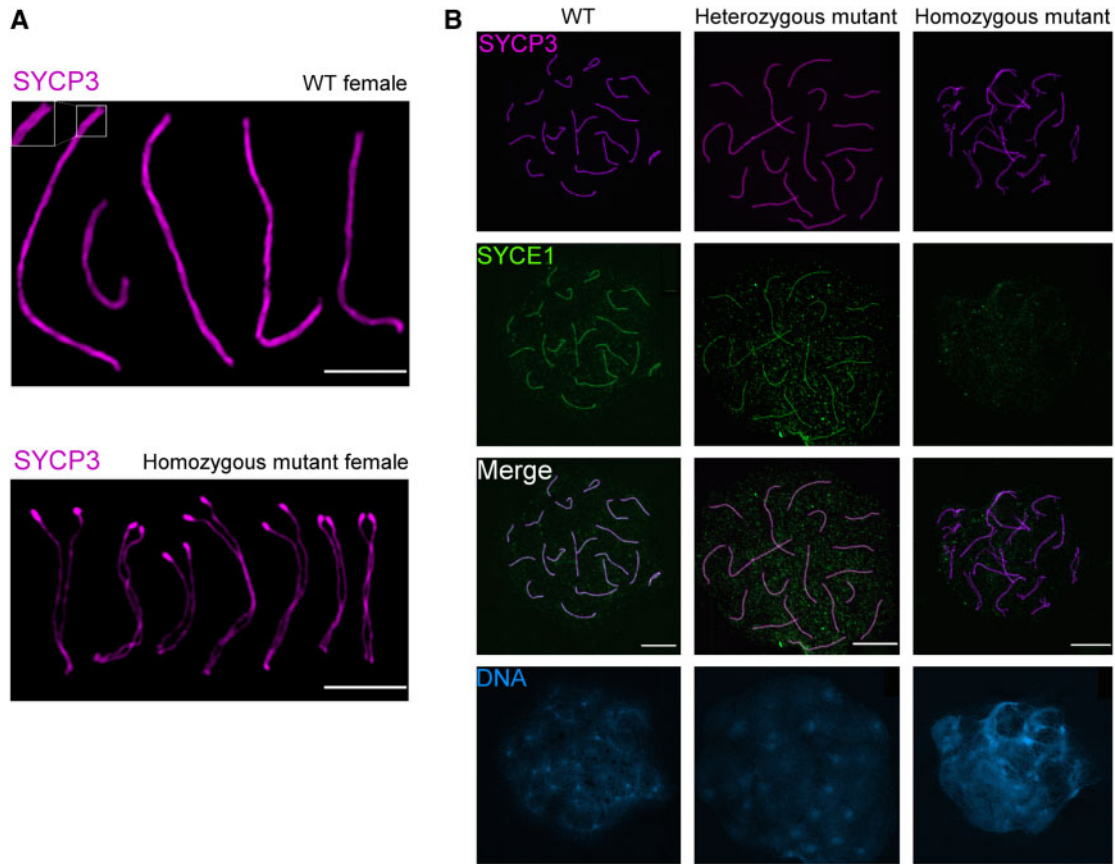


Figure 2. Evaluation of chromosome synapsis and SYCE1 loading to synaptonemal complex in WT and mutant mice. (A) Immunolabeling of LE component SYCP3 on spread meiotic chromosomes from WT (above) and homozygous mutant mice (below). Spread chromosomes from representative mice are shown stitched together. Fluorescence acquisition was performed by means of an Airyscan module that enabled the resolution of lateral elements (LEs), even in completely assembled synaptonemal complexes (SCs) (see inset above). Closely aligned but unsynapsed LEs are observed for homozygous mice (below). **(B)** Immunolocalization of SYCE1 protein in 18 dpc WT and mutant female mouse embryos. SYCE1 is shown in green, and SYCP3 in magenta. Merged channels and DNA staining with DAPI are also shown below. Bars correspond to 5 and 10 μm (A and B, respectively).

SYCP1 and SYCE3 fluorescence intensities were significantly lower for homozygous mutants as compared to WT littermates ($P < 0.0005$).

For spermatocytes, γH2AX was also immunolabeled along with SC protein components. This histone variant renders a very typical staining on male meiotic chromosomes: dispersed chromosome staining in early stages, then restricted to the XY body in pachytene stage. No difference in this regard was detected between WT and heterozygous male mutants (Fig. 3D). However, as expected for a pre-pachytene meiotic arrest, no restricted staining for the sexual chromosome pair was found in homozygous male mutants, which presented a diffuse γH2AX staining pattern, characteristic of earlier meiotic stages (Fig. 3D).

The putative truncated SYCE1 protein is not detected in mutant mice testes

Although no SYCE1 protein was detected on assembling SCs of homozygous mutant mice, still, the putative SYCE1 truncated protein could actually be present in meiocytes, but not incorporated into the SC. In order to shed some light on the molecular mechanism leading to

infertility, we assessed the presence of the putative truncated protein in mutant mice through western blot assays on testicular material. These protein studies cannot be performed in females due to material requirements unable to be fulfilled with embryonic ovaries (<0.0001 g).

A band with an apparent molecular mass of 38 KDa was detected both for WT mice and heterozygous mutants, in accordance with the predicted molecular weight for the WT 329-residue version of murine SYCE1 protein (Fig. 4A). No truncated SYCE1 protein (theoretical expected size: 28 KDa) was detected for heterozygous mutants.

Concerning homozygous mutants, no protein reactive to anti-SYCE1 antibody was detected at all (Fig. 4A). Protein gels were deliberately overloaded to minimize the effects of detection sensitivity limits, but in all assays no band of 28 KDa was observed.

Syce1 transcript is significantly decreased in humanized mice

The results from the western blot assays prompted us to analyze transcript levels. As shown in Fig. 4B, *Syce1* transcript quantification

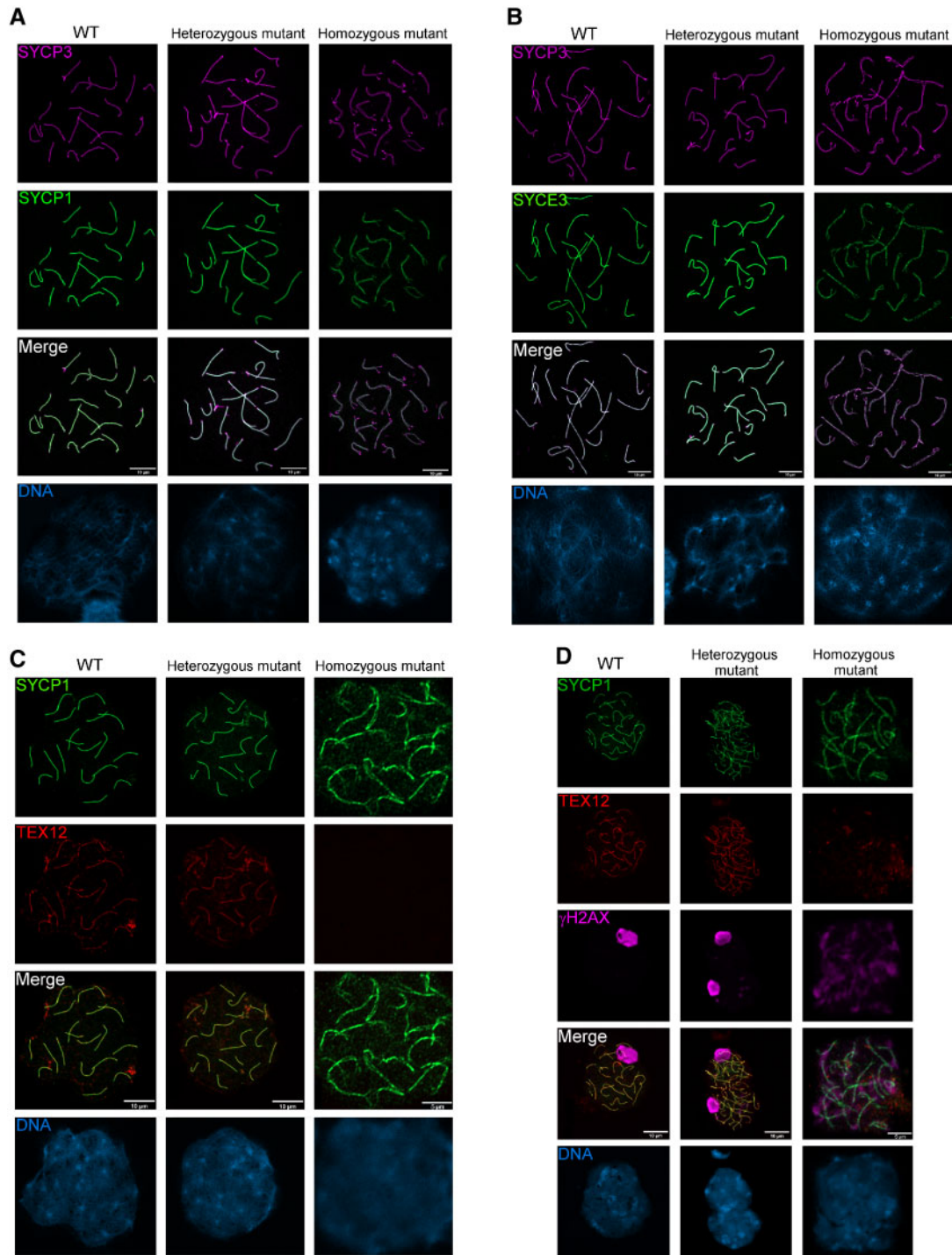


Figure 3. Immunolocalization of other CR SC components in WT and mutant mice. (A) Immunolabeling of TF SYCP1 in female 18 dpc mouse embryos. SYCP3 is shown in magenta and SYCP1 in green. (B) Immunolocalization of central element (CE) SYCE3 in female 18 dpc mouse embryos. SYCE3 is shown in green and SYCP3 in magenta. (C) Immunolabeling of CE TEX12 in female 18 dpc mouse embryos. SYCP1 is shown in green and TEX12 in red. (D) Immunolocalization of TEX12, SYCP1 and γ H2AX in male adult WT and mutant mice. SYCP1 is shown in green, TEX12 in red and γ H2AX (histone) in magenta. Merged channels and DNA staining with DAPI are shown below in each case.

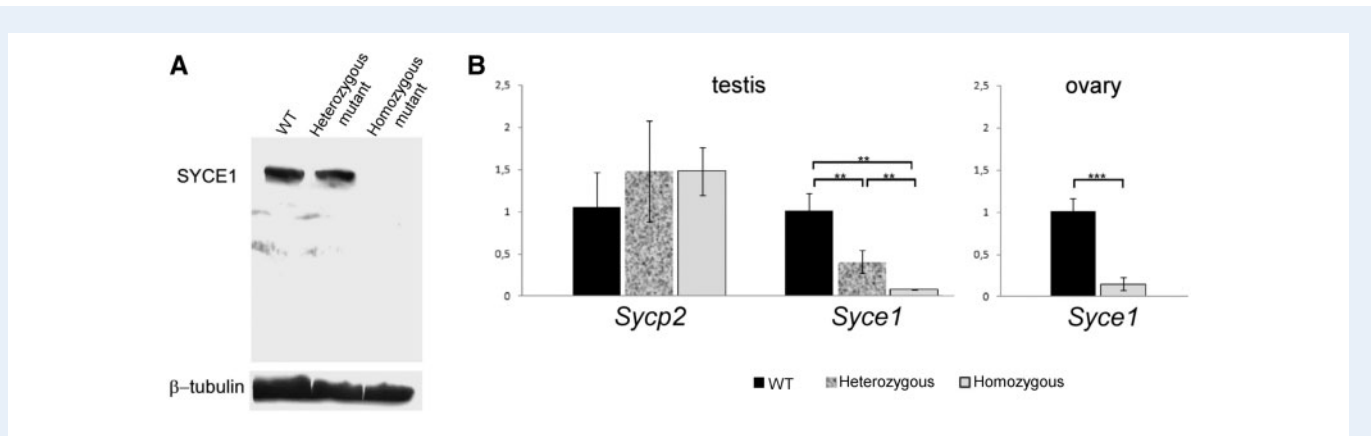


Figure 4. Analysis of SYCE1 protein by western blot, and transcript quantitation by quantitative RT-PCR. (A) Western blot analysis of SYCE1 protein and its putative truncated mutant variant in adult testes lysates from WT and mutant mice. The blotted bands were immunodetected with a specific rabbit antibody against mouse SYCE1 Nt-region. β -tubulin was employed as loading control. **(B)** Quantitative RT-PCR results obtained for adult testes and embryonic ovaries from WT and mutant mice ($n = 3$ for each category). SD (error bars), and statistical level of significance calculated by one-way ANOVA (horizontal bars) are indicated in each case. $**P < 0.005$; $***P < 0.0001$.

detected big differences between WT and homozygous mutants that exhibited minimum mRNA levels, both for embryonic ovaries ($P < 0.0001$) and for adult testes ($P < 0.005$).

Less pronounced but still significant differences were obtained between WT and heterozygous mutant males that showed intermediate transcript levels ($P < 0.01$; Fig. 4B). On the contrary and as expected, quantification of the *Sycp2* transcript (coding for SC LE SYCP2) revealed no significant differences between the three conditions.

Discussion

The present work relates to some POI cases that are presumably related to mutations in SC-coding genes, but still classified as idiopathic infertility. We have worked with the nonsense mutation *SYCE1* c.721C>T, addressing the question of its responsibility for the infertility observed in female patients homozygous for this mutation. We have also intended to shed some light on the underlying mechanisms involved. To achieve this, we have applied directed mutagenesis in the mouse for genome editing, and successfully generated a humanized mouse line (i.e. the edited murine genome contains a mutation equivalent to the one found in humans). In this regard, the high percentage of identity between human and mouse SYCE1 protein-coding genes allowed us to easily find an *SYCE1* c.721C>T murine equivalent mutation (*Syce1* c.727C>T). Generation of this animal model has enabled us to study the etiology and pathogenesis of POI.

Concerning etiology, it could be established that the homozygous presence of the *Syce1* c.727C>T mutation causes infertility in both female and male mice. This strongly suggests that the sole presence of the equivalent human mutation (*SYCE1* c.721C>T) in both alleles should be enough to produce the infertile phenotype observed in women (de Vries et al., 2014). On the other hand, mice heterozygous for the mutation were as fertile as WT mice. Thus, infertility in these cases would have a genetic origin and a recessive mode of inheritance. It is worth noting that for humans, de Vries and collaborators (i.e. the

authors that reported the mutation) found no clinical symptoms for heterozygous individuals of both genders examined in their study. However, the phenotype for homozygous males for the mutated *SYCE1* gene could not be known at that time because all the males examined in that study were found to be heterozygous for the mutation (de Vries et al., 2014). Thus, although the identification of this nonsense mutation was initially connected to cases of female infertility, we can now anticipate that the homozygous presence of this mutation would most probably cause infertility in men as well.

The fertility results reported here, demonstrate an absence of sexual dimorphism for this CE-related mutation. This would be in accordance with previous observations for mice with loss of function of CR component-coding genes, which are equally infertile in both genders (De Vries et al., 2005; Bolcun-Filas et al., 2007; Hamer et al., 2008; Bolcun-Filas et al., 2009; Schramm et al., 2011; Gómez-H et al., 2016), as opposed to LE-component mutants, which showed sexual dimorphism (Yuan et al., 2002; Yang et al., 2006).

Regarding gonadal development, the fact that we found no differences between heterozygous mutants and unaffected WT mice of both genders, is in accordance with the fertile phenotype observed in heterozygous humans, and also with our fertility tests results. On the other hand, the striking differences found in homozygous mutant gonads would explain their infertile phenotype. In particular, female mutant mice with an absence of recognizable oocytes and follicles (indicative of POI) resemble the clinical description of the human sisters who were homozygous for the mutation (de Vries et al., 2014), ratifying the validity of the experimental model.

In males, the seminiferous epithelium of homozygous mutants showed not only absence of postmeiotic cells, but also of midmeiotic prophase stages, thus indicating an early meiotic arrest. We also analyzed testicular cell suspensions by FCM as this methodology represents a widely accepted means to analyze testicular cellular content, with very high quantitative analytical power and statistical weight. These analyses corroborated a severely affected spermatogenic process in homozygous mutants, with testes completely depleted from

postmeiotic haploid cells with C DNA content (i.e. round and elongating spermatids, and spermatozoa). Moreover, concerning the 4C population (mainly composed of primary spermatocytes), FCM profiles obtained for homozygous mutants resembled those of ~13 dpp mice that have not reached the pachytene stage yet (Geisinger and Rodríguez-Casuriaga, 2017). This result is in agreement with the early meiotic arrest observed by microscopic examination.

Analysis of spread chromosomes immunolabeled against SC protein components, coupled to the use of an Airyscan super-resolution module, enabled assessment of chromosome synapsis, revealing that the homozygous presence of *Syce1* c.727C>T severely affects homologous synapsis. This provides a probable explanation for the lack of oocytes, as oocytes extensively defective in homolog synapsis would accumulate spontaneous DSBs and trigger the DNA damage checkpoint, leading to their elimination (Rinaldi et al., 2017).

Previous studies based on co-immunoprecipitation and yeast two-hybrid assays have identified SYCE1 interactions with SYCE3 and SIX6OS1 (Schramm et al., 2011; Lu et al., 2014; Gómez-H et al., 2016). Besides, SYCE1 recruitment to the SC has been proposed to be mediated by SYCE3 (Hernández-Hernández et al., 2016). While an SYCE3 immunolocalization signal was observed on SCs, neither SYCE protein nor SYCE1-downstream-loading SC components (e.g. TEX12) could be detected on meiotic chromosome axes of homozygous mutant mice. As the mutation under study is nonsense, two alternative hypotheses concerning the pathogenesis of these infertility cases arose: the putative SYCE1 truncated protein, which would lack 87 residues from the carboxyl terminus (Ct), would not be recruited and loaded to the SC as its interaction with SYCE3 would be impeded, thus affecting normal SC assembly after SYCE3 loading step; or SYCE1 loading disturbance could be due to absence of the putative truncated protein.

In order to shed some light on this matter, SYCE1 protein was assessed by western blot assays. The obtained results show the absence of detectable levels of the putative truncated protein both for the homozygous and for the heterozygous mutant mice, even in overloaded protein gels. This strongly suggests that the impeded synapsis phenotype observed in homozygous mutant mice would result from the absence (or at least presence of undetectable levels) of truncated SYCE1, thus supporting our second hypothesis above. Of note, the absence of an interfering shorter version of SYCE1 could explain the unaffected phenotype of heterozygous mutants. This would be quite different from the case of some *SYCP3* mutations where a dominant-negative effect has been reported in heterozygous patients, in which the truncated *SYCP3* interfered with polymerization of the normal protein (Miyamoto et al., 2003; Bolor et al., 2009). The lack of a possibly interfering truncated protein also has important implications concerning the development of eventual therapeutic procedures in homozygous mutant individuals, as it would guarantee the occurrence of no relevant interference with an eventually introduced exogenous normal protein, thus facilitating the intervention.

A possible mechanism involved in the lack of detectable mutant protein for this nonsense mutation could be nonsense-mediated mRNA decay (NMD). This regulatory pathway functions to degrade aberrant transcripts containing premature termination codons (PTCs). Since mutations that generate PTCs cause approximately one-third of all known human genetic diseases (Miller and Pearce, 2014), NMD has been proposed to have a potentially important role in human disease. The *SYCE1* c.721C>T mutation could be one of these cases. In order

to have a primary evaluation of this possibility, we have performed *Syce1* transcript quantitation in humanized mice compared to WT littermates. The results were consistent and pointed to transcript degradation of aberrant transcripts, with very low levels of transcript in homozygous mutant gonads of both genders. In addition, heterozygous mutant males showed intermediate *Syce1* levels, in accordance with NMD pathway involvement. Thus, the homozygous presence of *Syce1* c.727C>T mutation would lead—through a different mechanism—to a similar phenotype to that reported for *Syce1* KO mice, in which complete absence of SYCE1 protein causes infertility (Bolcun-Filas et al., 2009).

The findings reported here represent a proof of principle, since there are no previous reports on the employment of CRISPR/Cas technology to direct a specific change to an SC component, and generate a humanized mouse model line for its exhaustive study. Furthermore, the generated mouse model line can be further employed in other studies, including those aiming to develop eventual therapeutic procedures.

Supplementary data

Supplementary data are available at *Molecular Human Reproduction* online.

Acknowledgments

The authors wish to thank the staff of Transgenic and Experimental Animal Unit core facility from Institut Pasteur de Montevideo, Uruguay, for technical support in the generation of the GM model.

Authors' roles

D.H.L.: Mice genotyping, preparations for optical microscopy, spermatocyte spreading, protein immunolocalization experiments, western blot experiments, qRT-PCR from ovaries, statistical analysis, interpretation of results and manuscript correction. A.G.: Western blot experiments, data analysis, interpretation of results, critical discussion, manuscript correction and participation in the preparation of the revised version. M.F.T.: qRT-PCR experiments from testes and ovaries, data analysis, interpretation of results, critical discussion and manuscript correction. F.F.S.: Flow cytometric analysis, data analysis, interpretation of results, critical discussion and manuscript correction. M.B.: Embryonic ovaries dissection and spreading and manuscript correction. G.A.F.: Flow cytometric experimental design, data analysis, interpretation of results, critical discussion and manuscript correction. R.B.: Study conception, interpretation of results, critical discussion and manuscript correction. R.R.C.: Study conception and design, genome editing molecular design, study supervision, interpretation of results, critical discussion and manuscript preparation.

Funding

Funding for this research was provided by Agencia Nacional de Investigación e Innovación (ANII, Uruguay; <https://www.anii.org.uy/>),

grant number FCE-3-2016-1-126285 awarded to R.R.C., and fellowship POS_NAC_2018_1_151425 to D.H.L. Complementary financial support through program aliquots to R.R.C. and D.H.L. was provided by Programa de Desarrollo de las Ciencias Básicas (PEDECIBA, Biología), Universidad de la República (UdelaR). The funders had no role in study design, data collection and analysis, decision to publish or preparation of the manuscript.

Conflict of interest

All authors have no conflict of interest to declare.

References

- Alsheimer M, Baier A, Schramm S, Schutz W, Benavente R. Synaptonemal complex protein SYCP3 exists in two isoforms showing different conservation in mammalian evolution. *Cytogenet Genome Res* 2010;**128**:162–168.
- Bestetti I, Castronovo C, Sironi A, Caslini C, Sala C, Rossetti R, Crippa M, Ferrari I, Pistocchi A, Toniolo D et al. High-resolution array-CGH analysis on 46,XX patients affected by early onset primary ovarian insufficiency discloses new genes involved in ovarian function. *Hum Reprod* 2019;**34**:1–10.
- Bolcun-Filas E, Costa Y, Speed R, Taggart M, Benavente R, De Rooij DG, Cooke HJ. SYCE2 is required for synaptonemal complex assembly, double strand break repair, and homologous recombination. *J Cell Biol* 2007;**176**:741–747.
- Bolcun-Filas E, Speed R, Taggart M, Grey C, de Massy B, Benavente R, Cooke HJ. Mutation of the mouse *Syce1* gene disrupts synapsis and suggests a link between synaptonemal complex structural components and DNA repair. *PLoS Genet* 2009;**5**:e1000393.
- Bolor H, Mori T, Nishiyama S, Ito Y, Hosoba E, Inagaki H, Kogo H, Ohye T, Tsutsumi M, Takema K. Mutations of the *SYCP3* gene in women with recurrent pregnancy loss. *Am J Hum Genet* 2009;**84**:14–20.
- Chapman C, Cree L, Shelling AN. The genetics of premature ovarian failure: current perspectives. *Int J Womens Health* 2015;**7**:799–810.
- Costa Y, Speed R, Ollinger R, Alsheimer M, Semple CA, Gautier P, Maratou K, Novak I, Hoog C, Benavente R et al. Two novel proteins recruited by synaptonemal complex protein I (SYCP1) are at the centre of meiosis. *J Cell Sci* 2005;**118**:2755–2762.
- Coulam CB, Stringfellow S, Hoefnagel D. Evidence for a genetic factor in the etiology of premature ovarian failure. *Fertil Steril* 1983;**40**:693–695.
- Crispo M, Schlapp G, Cárdenas-Rodríguez M, González-Maciél D, Rumbo M. Optimization of transgenesis conditions for the generation of CXCL2-luciferase reporter mice line. *Electron J Biotechnol* 2013;**16**:14.
- da Cruz I, Rodríguez-Casuriaga R, Santiñaque FF, Farías J, Curti G, Capoano CA, Folle GA, Benavente R, Sotelo-Silveira JR, Geisinger A. Transcriptome analysis of highly purified mouse spermatogenic cell populations: gene expression signatures switch from meiotic-to postmeiotic-related processes at pachytene stage. *BMC Genomics* 2016;**17**:294–312.
- De Vries L, Behar DM, Smirin-Yosef, P, Lagovsky, I, Tzur, S, Basel-Vanagaite, L. Exome sequencing reveals *SYCE1* mutation associated with autosomal recessive primary ovarian insufficiency. *J Clin Endocrinol Metab* 2014;**99**:2129–2132.
- De Vries FA, de Boer E, van den Bosch M, Baarends WM, Ooms M, Yuan L, Liu JG, van Zeeland AA, Heyting C, Pastink A. Mouse *Sycp1* functions in synaptonemal complex assembly, meiotic recombination, and XY body formation. *Genes Dev* 2005;**19**:1376–1389.
- Di Pasquale E, Rossetti R, Marozzi A, Bodega B, Borgato S, Cavallo L, Einaudi S, Radetti G, Russo G, Sacco M et al. Identification of new variants of human *BMP15* gene in a large cohort of women with premature ovarian failure. *J Clin Endocrinol Metab* 2006;**91**:1976–1979.
- Doherty E, Pakarinen P, Tiitinen A, Kiilavuori A, Huhtaniemi I, Forrest S, Aittomäki K. A novel mutation in the FSH receptor inhibiting signal transduction and causing primary ovarian failure. *J Clin Endocrinol Metab* 2002;**87**:1151–1155.
- Ennis S, Ward D, Murray A. Nonlinear association between CGG repeat number and age of menopause in *FMR1* premutation carriers. *Eur J Hum Genet* 2006;**14**:253–255.
- Fraune J, Schramm S, Alsheimer M, Benavente R. The mammalian synaptonemal complex: protein components, assembly and role in meiotic recombination. *Exp Cell Res* 2012;**318**:1340–1346.
- Fonseca J, Patino LC, Suárez Y, Rodríguez J, Mateus H, Jiménez K, Ortega-Recalde O, Díaz-Yamal I, Laissue P. Next generation sequencing in women affected by nonsyndromic premature ovarian failure displays new potential causative genes and mutations. *Fertil Steril* 2015;**104**:154–162.e2.
- Geisinger A, Benavente R. Mutations in genes coding for synaptonemal complex proteins and their impact on human fertility. *Cytogenet Genome Res* 2016;**150**:77–85.
- Geisinger A, Rodríguez-Casuriaga R. Flow cytometry for the isolation and characterization of rodent meiocytes. *Methods Mol Biol* 2017;**1471**:217–230.
- Glauert AM, Lewis PR. Biological specimen preparation for transmission electron microscopy. In: Glauert AM (ed). *Practical Methods in Electron Microscopy*, Vol. **17**. London: Portland Press, 1998.
- Goldman A, Rodríguez-Casuriaga R, González-López E, Capoano CA, Santiñaque FF, Geisinger A. MTCH2 is differentially expressed in rat testis and mainly related to apoptosis of spermatocytes. *Cell Tissue Res* 2015;**361**:869–883.
- Gómez-H L, Felipe-Medina N, Sánchez-Martín M, Davies OR, Ramos I, García-Tuñón I, de Rooij DG, Dereli I, Tóth A, Barbero JL et al. C14ORF39/SIX6OS1 is a constituent of the synaptonemal complex and is essential for mouse fertility. *Nat Commun* 2016;**7**:13298.
- Goswami D, Conway GS. Premature ovarian failure. *Hum Reprod Update* 2005;**11**:391–410.
- Hamer G, Gell K, Kouznetsova A, Novak I, Benavente R, Hoog C. Characterization of a novel meiosis-specific protein within the central element of the synaptonemal complex. *J Cell Sci* 2006;**119**:4025–4032.
- Hamer G, Wang H, Bolcun-Filas E, Cooke H. J, Benavente R, Hoog C. Progression of meiotic recombination requires structural maturation of the central element of the synaptonemal complex. *J Cell Sci* 2008;**121**:2445–2451.
- Hernández-Hernández A, Masich S, Fukuda T, Kouznetsova A, Sandin S, Daneholt B, Höög C. The central element of the

- synaptonemal complex in mice is organized as a bilayered junction structure. *J Cell Sci* 2016;**129**:2239–2249.
- Huhtaniemi I, Hovatta O, La Marca A, Livera G, Monniaux D, Persani L, Heddar A, Jarzabek K, Laisk-Podar T, Salumets A et al. Advances in the molecular pathophysiology, genetics, and treatment of primary ovarian insufficiency. *Trends Endocrinol Metab* 2018;**29**:400–419.
- Laissue P. Aetiological coding sequence variants in non-syndromic premature ovarian failure: from genetic linkage analysis to next generation sequencing. *Mol Cell Endocrinol* 2015;**411**:243–257.
- Laissue P, Christin-Maitre S, Touraine P, Kuttann F, Ritvos O, Aittomaki K, Bourcigaux N, Jacquesson L, Bouchard P, Frydman R et al. Mutations and sequence variants in *GDF9* and *BMP15* in patients with premature ovarian failure. *Eur J Endocrinol* 2006;**154**:739–744.
- Lammers JH, Offenberg HH, Van Aalderen M, Vink AC, Dietrich AJ, Heyting C. The gene encoding a major component of the lateral elements of synaptonemal complexes of the rat is related to X-linked lymphocyte-regulated genes. *Mol Cell Biol* 1994;**14**:1137–1146.
- Livak KJ, Schmittgen TD. Analysis of relative gene expression data using real-time quantitative PCR and the $2^{-\Delta\Delta C(T)}$ method. *Methods* 2001;**25**:402–408.
- Lu J, Gu Y, Feng J, Zhou W, Yang X, Shen Y. Structural insight into the central element assembly of the synaptonemal complex. *Sci Rep* 2014;**4**:7059.
- Maor-Sagie E, Cinnamon Y, Yaacov B, Shaag A, Goldsmid H, Zenvirt S, Laufer N, Richler C, Frumkin A. Deleterious mutation in *SYCE1* is associated with non-obstructive azoospermia. *J Assist Reprod Genet* 2015;**32**:887–891.
- Matsudaira P. Sequence from picomole quantities of proteins electro-blotted onto polyvinylidene difluoride membranes. *J Biol Chem* 1987;**262**:10035–10038.
- McGuire MM, Bowden W, Engel NJ, Ahn HW, Kovanci E, Rajkovic A. Genomic analysis using high-resolution single-nucleotide polymorphism arrays reveals novel microdeletions associated with premature ovarian failure. *Fertil Steril* 2011;**95**:1595–1600.
- Meuwissen RL, Offenberg HH, Dietrich AJ, Riesewijk A, Van Iersel M, Heyting C. A coiled-coil related protein specific for synapsed regions of meiotic prophase chromosomes. *EMBO J* 1992;**11**:5091–5100.
- Miller JN, Pearce DA. Nonsense-mediated decay in genetic disease: friend or foe? *Mutat Res Rev Mutat Res* 2014;**762**:52–64.
- Miyamoto T, Hasuike S, Yogeve L, Maduro MR, Ishikawa M, Westphal H, Lamb DJ. Azoospermia in patients heterozygous for a mutation in *SYCP3*. *Lancet* 2003;**362**:1714–1749.
- National Research Council (NRC). *Guide for the Care and Use of Laboratory Animals*, 7th edn. Washington, DC: National Academies Press, 1996.
- Offenberg HH, Schalk JA, Meuwissen RL, Van Aalderen M, Kester HA, Dietrich AJ, Heyting C. SCP2: a major protein component of the axial elements of synaptonemal complexes of the rat. *Nucleic Acids Res* 1998;**26**:2572–2579.
- Pagnamenta T, Taanman W, Wilson C, Anderson N, Marotta R, Duncan A, Bitner-Glindzic M, Taylor R, Laskowski A, Thorburn D. Dominant inheritance of premature ovarian failure associated with mutant mitochondrial DNA polymerase gamma. *Hum Reprod* 2006;**21**:2467–2473.
- Pashaei M, Rahimi Bidgoli MM, Zare-Abdollahi D, Najmabadi H, Haji-Seyed-Javadi R, Fatehi F, Alavi A. The second mutation of *SYCE1* gene associated with autosomal recessive nonobstructive azoospermia. *J Assist Reprod Genet* 2020;**37**:451–458.
- Peters AH, Plug AW, van Vugt MJ, de Boer P. A drying-down technique for the spreading of mammalian meiocytes from the male and female germline. *Chromosome Res* 1997;**5**:66–68.
- Qin Y, Choi Y, Zhao H, Simpson JL, Chen ZJ, Rajkovic A. *NOBOX* homeobox mutation causes premature ovarian failure. *Am J Hum Genet* 2007;**81**:576–581.
- Rinaldi VD, Bolcun-Filas E, Kogo H, Kurahashi H, Schimenti JC. The DNA damage checkpoint eliminates mouse oocytes with chromosome synapsis failure. *Mol Cell* 2017;**67**:1026–1036.
- Riva P, Magnani I, Fuhrmann Conti AM, Gelli D, Sala C, Toniolo D, Larizza L. FISH characterization of the Xq21 breakpoint in a translocation carrier with premature ovarian failure. *Clin Genet* 1996;**50**:267–269.
- Rodríguez-Casuriaga R, Folle GA, Santiñaque F, López-Carro B, Geisinger A. Simple and efficient technique for the preparation of testicular cell suspensions. *J Vis Exp* 2013;**78**:e50102.
- Rodríguez-Casuriaga R, Geisinger A, López-Carro B, Porro V, Wettstein R, Folle GA. Ultra-fast and optimized method for the preparation of rodent testicular cells for flow cytometric analysis. *Biol Proced Online* 2009;**11**:184–195.
- Rodríguez-Casuriaga R, Santiñaque F, Folle GA, López-Carro B, Geisinger A. Rapid preparation of rodent testicular cell suspensions and spermatogenic stages purification by flow cytometry using a novel blue-laser-excitable vital dye. *MethodsX* 2014;**1**:239–243.
- Schillit SLP, Menon S, Friedrich C, Kammin T, Wilch E, Hanscom C, Jiang S, Kliesch S, Talkowski ME, Tüttelmann F et al. *SYCP2* translocation-mediated dysregulation and frameshift variants cause human male infertility. *Am J Hum Genet* 2020;**106**:41–57.
- Schindelin J, Arganda-Carreras I, Frise E, Kaynig V, Longair M, Pietzsch T, Preibisch S, Rueden C, Saalfeld S, Schmid B et al. Fiji: an open-source platform for biological-image analysis. *Nat Methods* 2012;**9**:676–682.
- Schlapp G, Goyeneche L, Fernández G, Menchaca A, Crispo M. Administration of the nonsteroidal anti-inflammatory drug tolfenamic acid at embryo transfer improves maintenance of pregnancy and embryo survival in recipient mice. *J Assisted Reprod Genet* 2015;**32**:271–275.
- Schramm S, Fraune J, Naumann R, Hernández-Hernández A, Hoog C, Cooke HJ, Alsheimer M, Benavente R. A novel mouse synaptonemal complex protein is essential for loading of central element proteins, recombination, and fertility. *PLoS Genet* 2011;**7**:e1002088.
- Schücker K, Holm T, Franke C, Sauer M, Benavente R. Elucidation of synaptonemal complex organization by super-resolution imaging with isotropic resolution. *Proc Natl Acad Sci USA* 2015;**112**:2029–2033.
- Tran TN, Martínez J, Schimenti JC. A predicted deleterious allele of the essential meiosis gene *MND1*, present in ~3% of East Asians, does not disrupt reproduction in mice. *Mol Hum Reprod* 2019;**25**:668–673.

- Tran TN, Schimenti JC. A putative human infertility allele of the meiotic recombinase DMC1 does not affect fertility in mice. *Hum Mol Genet* 2018;**27**:3911–3918.
- Tran TN, Schimenti JC. A segregating human allele of *SPO11* modeled in mice disrupts timing and amounts of meiotic recombination, causing oligospermia and a decreased ovarian reserve. *Biol Reprod* 2019;**101**:347–359.
- Van Kasteren YM, Schoemaker J. Premature ovarian failure: a systematic review on therapeutic interventions to restore ovarian function and achieve pregnancy. *Hum Reprod Update* 1999;**5**:483–492.
- Watkins WJ, Umbers AJ, Woad KJ, Harris SE, Winship IM, Gersak K, Shelling AN. Mutational screening of *FOXO3A* and *FOXO1A* in women with premature ovarian failure. *Fertil Steril* 2006;**86**:1518–1521.
- Winkel K, Alsheimer M, Ollinger R, Benavente R. Protein SYCP2 provides a link between transverse filaments and lateral elements of mammalian synaptonemal complexes. *Chromosoma* 2009;**118**:259–267.
- Yang F, De La Fuente R, Leu NA, Baumann C, McLaughlin KJ, Wang PJ. Mouse SYCP2 is required for synaptonemal complex assembly and chromosomal synapsis during male meiosis. *J Cell Biol* 2006;**173**:497–507.
- Yang L, Guell M, Byrne S, Yang JL, De Los Angeles A, Mali P, Aach J, Kim-Kiselak C, Briggs AW, Rios X et al. Optimization of scarless human stem cell genome editing. *Nucleic Acids Res* 2013;**41**:9049–9061.
- Yuan L, Liu JG, Hoja MR, Wilbertz J, Nordqvist K, Hoog C. Female germ cell aneuploidy and embryo death in mice lacking the meiosis-specific protein SCP3. *Science* 2002;**296**:1115–1118.
- Zhao H, Chen ZJ, Qin Y, Shi Y, Wang S, Choi Y, Simpson JL, Rajkovic A. Transcription factor FIGLA is mutated in patients with premature ovarian failure. *Am J Hum Genet* 2008;**82**:1342–1348.
- Zhe J, Ye D, Chen X, Liu Y, Zhou X, Li Y, Zhang J, Chen S. Consanguineous Chinese familial study reveals that a gross deletion that includes the *SYCE1* gene region is associated with premature ovarian insufficiency. *Reprod Sci* 2020;**27**:461–467.
- Zhen XM, Sun YM, Qiao J, Li R, Wang LN, Liu P. Genome-wide copy number scan in Chinese patients with premature ovarian failure. *Beijing Da Xue Xue Bao* 2013;**45**:841–847.
- Zickler D, Kleckner N. Recombination, pairing, and synapsis of homologs during meiosis. *Cold Spring Harb Perspect Biol* 2015;**7**:1–26.cshperspect.a016626.